

Policy Perturbation via Noisy Advantage Values for Cooperative Multi-agent Actor-Critic methods

Jian Hu^{**}

National Taiwan University
Taipei, Taiwan
janhu9527@gmail.com

Weixun Wang

Tianjin University
Tianjin, China Mainland
wxwang@tju.edu.cn

Siyue Hu^{*}

National Taiwan University
Taipei, Taiwan
husiyuehusiyue@gmail.com

Shih-wei Liao

National Taiwan University
Taipei, Taiwan
liao24@gmail.com

ABSTRACT

Multi-Agent Reinforcement Learning (MARL) has seen revolutionary breakthroughs with its successful application to multi-agent cooperative tasks such as robot swarms control, autonomous vehicle coordination, and computer games. Recent works have applied the Proximal Policy Optimization (PPO) to the multi-agent tasks, such as Independent PPO (IPPO); and vanilla Multi-agent PPO (MAPPO) which has a centralized value function. However, previous literature shows that MAPPO may not perform as well as Independent PPO (IPPO) and the Fine-tuned QMIX. Thus MAPPO-Feature-Pruned (MAPPO-FP) further improves the performance of MAPPO by the carefully designed artificial features. In addition, there is no literature that gives a theoretical analysis of the working mechanism of MAPPO. In this paper, we firstly theoretically generalize single-agent PPO to the vanilla MAPPO, which shows that the vanilla MAPPO is approximately equivalent to optimizing a multi-agent joint policy with the original PPO. Secondly, we find that MAPPO faces the problem of *The Policies Overfitting in Multi-agent Cooperation (POMAC)*, as they learn policies by the sampled centralized advantage values. Then POMAC may lead to updating the policies of some agents in a suboptimal direction and prevent the agents from exploring better trajectories. To solve the POMAC, we propose two novel policy perturbation methods, i.e., Noisy-Value MAPPO (NV-MAPPO) and Noisy-Advantage MAPPO (NA-MAPPO), which disturb the advantage values via random Gaussian noise. The experimental results show that the performance of our methods is better than that of Fine-tuned QMIX and MAPPO-FP, and achieves SOTA in Starcraft Multi-Agent Challenge (SMAC). We open-source the code at <https://github.com/hijkzzz/noisy-mappo>.

KEYWORDS

Multi-agent, Reinforcement Learning, Noise, PPO

ACM Reference Format:

Jian Hu^{**}, Siyue Hu^{*}, Weixun Wang, and Shih-wei Liao. 2022. Policy Perturbation via Noisy Advantage Values for Cooperative Multi-agent Actor-Critic methods. In *preprint*, , , IFAAMAS, 12 pages.

^{*} Jian Hu and Siyue Hu contributed equally to this work.

^{**} Corresponding Author.

1 INTRODUCTION

Multi-Agent Reinforcement Learning (MARL) has seen revolutionary breakthroughs with its successful application to multi-agent cooperative tasks such as robot swarms control [6], autonomous vehicle coordination [1] and computer games [19]. As for scalability and communication security problems, decentralized execution of multi-agent policies that act only on their local observations is widely used. An intuitive approach for decentralized multi-agent policy learning is the Independent Q Learning (IQL) [24]. However, IQL does not address the non-stationarity introduced due to the changing policies of the learning agents. Thus, unlike single-agent Reinforcement Learning (RL) algorithms, there is no guarantee of convergence even at the limit of infinite exploration. Therefore, the *Centralized Training and Decentralized Execution (CTDE)* [10], which allows for agent to access global information during training stage, is widely used in MARL algorithms [13, 18].

Many CTDE algorithms, e.g. MADDPG [13], MAAC [7], QMIX [18], have been proposed for multi-agent cooperative tasks. Among these algorithms, the finetuned QMIX [5] achieves the SOTA performance in the popular MARL benchmark environment Starcraft Multi-Agent Challenge(SMAC) [19]. To enable effective CTDE for multi-agent Q-learning, the Individual-Global-Max (IGM) principle [22] of equivalence of joint greedy action and individual greedy actions is critical. QMIX ensures that the IGM condition holds by the mixing network with *Monotonicity Constraint* [18]. However, the mixing network leads to limitations in its scalability, and monotonicity constraints prevent it from learning correctly in non-monotonic environments [22]. We turn our attention to the efficient single-agent RL algorithms, such as Trust Region Policy Optimization (TRPO) [20] and Proximal Policy Optimization (PPO) [21], as their unlimited expressive power and high sample efficiency.

Recently, the literature [3] applies the PPO to the multi-agent tasks directly, called Independent PPO (IPPO); literature [3] also extend IPPO to the vanilla Multi-agent PPO (MAPPO) which using the centralized value function. However, the MAPPO may not perform as well as Independent PPO (IPPO) and the Fine-tuned QMIX [5]. Then literature [26] further improves the performance of vanilla MAPPO and IPPO by carefully designed agent-specific features, called MAPPO-Feature-Pruned (MAPPO-FP) (details in Sec. 3); literature [11] proposed a multi-agent TRPO algorithm, but only for the case where each agent has a private reward. In addition, there is no literature that gives a theoretical analysis for the working

mechanism of MAPPO in multi-agent settings. By contrast, we find that vanilla MAPPO faces the problem of *The Policies Overfitting in Multi-agent Cooperation(POMAC)* as they learn policies by the sampled centralized advantage values [15]. Then POMAC may lead to updating the policies of some agents in a suboptimal direction and prevent the agents from exploring better trajectories.

In this paper, (1) We extend single-agent PPO to Multi-agent PPO (MAPPO) from a theoretical perspective, which shows that MAPPO is approximately equivalent to optimizing a multi-agent joint policy with the original PPO. (2) To solve the POMAC, we propose novel policy perturbation methods, i.e, Noisy-Value MAPPO (NV-MAPPO) and Noisy-Advantage MAPPO (NA-MAPPO), which disturb the advantage values via random Gaussian noise. (3) Empirical results show that our approaches achieve better performance than the Fine-tuned QMIX [5], MAPPO-FP [26], and is much better than MAPPO (Sec. 6 and Appendix C.1), **without artificial agent-specific features**.

We are the first to propose to improve the effectiveness of the Multi-agent Actor-Critic algorithms by policies perturbation with noisy advantage values.

2 BACKGROUND

Dec-POMDP We consider a cooperative task, which can be described as a decentralized partially observable Markov decision process (Dec-POMDP)[16]. The cooperative agent chooses sequential actions under partial observation and environment stochasticity. Dec-POMDP is a tuple $(\mathcal{S}, \mathcal{A}, \mathcal{O}, \mathcal{R}, \mathcal{P}, n, \gamma)$ where \mathcal{S} is state space. \mathcal{A} is joint action space. $o_i = \mathcal{O}(s; i)$ is partially observation for agent i at global state s . $\mathcal{P}(s'|s, \mathcal{A})$ is the state transition probability in the environment given the joint action $\mathcal{A} = (a_1, \dots, a_N)$. Every agent has same shared reward function $\mathcal{R}(s, \mathcal{A})$. N denotes the number of agents and $\gamma \in [0, 1)$ is the discount factor. The team of agents attempt to learn a joint policy $\pi = \langle \pi_1, \dots, \pi_N \rangle$ that maximises their expected discounted return.

$$V^\pi(s_0) = \mathbb{E}_{a^1 \sim \pi^1, \dots, a^N \sim \pi^N, s \sim T} \left[\sum_{t=0}^{\infty} \gamma^t r_t \left(s_t, a_t^1, \dots, a_t^N \right) \right] \quad (1)$$

CTDE Centralized training with decentralized execution(CTDE) paradigm[10], in which agents can obtain additional information and centralized joint learning; while in the testing phase, agents make the decision based on their own partially observation. Next, we introduce some CTDE algorithms for the multi-agent credit assignment [2].

Credit assignment Multi-agent credit assignment [2] is a critical challenge: in cooperative settings, joint actions typically generate only global rewards, making it difficult for each agent to deduce its own contribution to the team's success. Many CTDE algorithms have been proposed to solve this problem: COMA [4] trains decentralized agents by a centralized critic with counterfactual advantages. MADDPG [13] and MAAC [7] trains a joint critic to extend DDPG [12] to the multi-agent setting, which can be seen as implicit credit assignment [27]. VDN [23], QMIX [18] (details in Sec. 3) decompose the joint action-value function Q_{tot} to individual action-value functions Q_i by the value mixing networks. However, the monotonicity constraints limit the expressive

power of QMIX, which may learn error argmax action in nonmonotonic cases [22] [14]. Besides, we consider a task including millions of agents, but only several states, the mixing network faces the problem of explosion in the size of Q_i .

Policy Gradient (PG) Then, we briefly introduce the Policy Gradient (PG) and Proximal Policy Optimization (PPO) in single-agent RL. In the on-policy case, the gradient of the object value function $V^\pi(s_0) \stackrel{\text{def}}{=} \mathbb{E}_\pi \left[\sum_{t \geq 0} \gamma^t r_t \right]$, where $\gamma \in [0, 1)$ with respect to some parameter of the policy π is

$$\nabla V^\pi(s_0) = \mathbb{E}_\pi \left[\sum_{t \geq 0} \gamma^t \nabla \log \pi(a_t | s_t) A^\pi(s_t, a_t) \right] \quad (2)$$

where $A^\pi(s_t, a_t) := Q^\pi(s_t, a_t) - V^\pi(s_t)$ is the advantage value function [15] of policy π , where $Q^\pi(s_t, a_t) := r_t + \gamma V^\pi(s_{t+1})$ is the state action value function. Intuitively, PG makes the policy π closer to the actions with large advantage value by gradient ascending.

Proximal Policy Optimization (PPO) To improve the sample efficiency of PG, Trust Region Policy Optimization (TRPO) [20] aims to maximize the objective function $V^\pi(s_0)$ subject to, trust region constraint which enforces the distance between old and new policies measured by KL-divergence to be small enough, within a parameter δ ,

$$J^{TRPO} = \mathbb{E}_{a_t, s_t \sim \pi_{old}} \left[\frac{\pi(a_t | s_t)}{\pi_{old}(a_t | s_t)} A^{\pi_{old}}(s_t, a_t) \right] \quad (3)$$

where $\frac{\pi(a_t | s_t)}{\pi_{old}(a_t | s_t)}$ is the Importance sampling (IS) weight, with KL-divergence constraint,

$$\mathbb{E}_{s \sim \rho^{\pi_{old}}} \left[D_{KL} \left(\pi_{\theta_{old}}(\cdot | s) \| \pi_{\theta}(\cdot | s) \right) \right] \leq \delta \quad (4)$$

where $\rho^{\pi_{old}}$ is the discounted state distribution [20] sampled by policy π_{old} . [20] prove that J^{TRPO} is equivalent to the Natural Policy Gradient (NPG) [8], which enable the the gradient in the steepest direction of object function. However, in large-scale neural networks, the KL-divergence constraint causes the objective function to be difficult to solve. Therefore, PPO-clip [21] proposes an approximate objective function (Eq. 6),

$$r = \frac{\pi(a | s)}{\pi_{old}(a | s)} \quad (5)$$

$$J^{PPO-clip} = \mathbb{E}_{a_t, s_t \sim \pi_{old}} \left[\min \left(r A^{\text{old}}(s, a), \text{clip}(r, 1 - \epsilon, 1 + \epsilon) A^{\text{old}}(s, a) \right) \right] \quad (6)$$

The function $\text{clip}(r, 1 - \epsilon, 1 + \epsilon)$ clips the ratio to be no more than $1 - \epsilon$ and no less than $1 + \epsilon$, which approximates the KL-divergence constraint.

3 RELATED WORKS

In this section we briefly introduce some related work, such as Independent PPO (IPPO), MAPPO-Feature-Pruned [26] and multi-agent TRPO [11].

Indepent PPO (IPPO) & Non-stationarity IPPO train an independent PPO agent for each agent in the multi-agent system, and the literature [3] shows that he works effectively as well in some multi-agent tasks. However, applying the single-agent policy

gradient algorithms to the multi-agent faces the problem of environmental **non-stationarity**. Specifically, for a certain agent i in a multi-agent system, we can treat other agents' policies as part of the environment; then, the Bellman Equation is

$$V^{\pi^i}(s) = \sum_a \pi^i(a^i | s) \sum_{s',r} p(s',r | s, a^i, \vec{\pi}^-) (r + v_{\pi^i}(s')) \quad (7)$$

where $p(s',r | s, a, \vec{\pi}^-)$ is the state transition function in the multi-agent setting, and $\vec{\pi}^-$ denotes the policies of other agents. Since the policy of each agent is updated synchronously, the state transition function p is non-stationary, and thus the convergence of the Bellman Equation cannot be guaranteed.

vanilla MAPPO extends IPPO's independent critics to a centralized critic with global information s . As for the global information, the centralized critic is more accurate than the independent critics. However, literature [3] demonstrates that he does not work well in complex environments.

MAPPO-Feature-Pruned (MAPPO-FP) [26] finetunes the hyperparameters of vanilla MAPPO to enable it to perform well in complex multi-agent tasks such as SMAC. **MAPPO-FP feeds well-designed artificial features (agent-specific features) to the critic networks**, which significantly improved MAPPO's performance in SMAC. The agent-specific features (shown in Figure 1) concatenate the global state s with agent-specific information, such as agent actions mask and agent's information.



Figure 1: MAPPO-FP concatenates artificially designed agent's information with global state.

In addition, all these works related to multi-agent PPO do not give a theoretical analysis about the MAPPO and its working mechanism.

multi-agent TRPO Recently, [11] propose a multi-agent TRPO algorithm with a theoretical analysis. However, this algorithm can only optimize decentralized policies based on local observations and **private rewards** for each agent, which may not be suitable for complex cooperative tasks with shared rewards. Our method only needs the shared reward without credit assignment.

4 MULTI-AGENT POLICY GRADIENT

In this section, we extend the single-agent policy gradient to multi-agent policy-gradient from the theoretical perspective, which shows that **the vanilla MAPPO is approximately equivalent to optimizing a joint policy with PPO**.

Joint Policy Modeling To solve non-stationary problem, we model all agents' policies as a joint policy. i.e, we consider the joint policy with N agents, likewise that of COMA [4],

$$\pi(\vec{a} | s) \approx \prod_i^N \pi^i(a^i | s) \quad (8)$$

$$\approx \prod_i^N \pi^i(a^i | \tau^i) \quad (9)$$

If actions and observations history τ^i contains enough information for right decisions, i.e, the agent can infer the actions of other agents and other information it needs through τ^i , the above Eq. 9 holds equivalently. This joint policy treats all agents as a super-agent, thus avoids introducing other agents' policies in the state transition function p , in effect obviating the non-stationary. We note that all sub-policies depend on the same state s , so they are not completely independent.

Multi-agent PG (MAPG) Then, we put the Eq. 9 into Eq. 2 to simplify the PG formula,

$$\begin{aligned} g &= \mathbb{E}_{a_t, s_t \sim \pi} [\nabla \log \pi(\vec{a}_t | s_t) A(s_t, \vec{a}_t)] \\ &\approx \mathbb{E}_{a_t, s_t \sim \pi} \left[\nabla \log \prod_i^N \pi^i(a_t^i | \tau_t^i) A(s_t, \vec{a}_t) \right] \\ &= \sum_i^N \mathbb{E}_{a_t, s_t \sim \pi} \left[\nabla \log \pi^i(a_t^i | \tau_t^i) A(s_t, \vec{a}_t) \right] \end{aligned} \quad (10)$$

Eq. 10 shows that we can optimize the decentralized policies using the single-agent PG gradient, with a centralized advantage function. This implies that we use the shared centralized advantage values as

$$A^\pi(s_t, a_t) = r_t + \gamma V^\pi(s_{t+1}) - V^\pi(s_t) \quad (11)$$

and fortunately, CTDE allows us to train a central value function using global information s .

Multi-agent PPO (MAPPO) Intuitively, we can directly use the PPO (Eq. 6) to optimize the multi-agent joint policy (Eq. 9) likewise MAPG, i.e,

$$r^m = \prod_i^N \frac{\pi^i(a^i | \tau^i)}{\pi_{old}^i(a^i | \tau^i)} \quad (12)$$

$$J = \mathbb{E}_{a_t, s_t \sim \pi^{old}} \left[\min \left(r^m A^{old}(s, a), \text{clip}(r^m, 1 - \epsilon, 1 + \epsilon) A^{old}(s, \vec{a}) \right) \right] \quad (13)$$

By contrast, we show a surrogate objective function that is suitable for multi-agent settings: since the KL-divergence is additive for independent distributions in much the same way as Shannon entropy; The KL-divergence constraint (Eq. 4) between the joint policy π_{old} and π ,

$$\mathbb{E}_{s \sim \rho^{\pi_{old}}} \left[D_{KL} \left(\prod_i^N \pi_{old}^i(\cdot | s) \| \prod_i^N \pi^i(\cdot | s) \right) \right] \leq \delta. \quad (14)$$

can be simplified as ¹,

$$\mathbb{E}_{s \sim \rho^{\pi_{old}}} \left[\sum_i^N D_{KL} \left(\pi_{old}^i(\cdot | s) \| \pi^i(\cdot | s) \right) \right] \leq \delta. \quad (15)$$

Therefore, we just need the following constraint for each agent i to hold,

$$\mathbb{E}_{s \sim \rho^{\pi_{old}}} \left[D_{KL} \left(\pi_{\theta_{old}}^i(\cdot | \tau^i) \| \pi^i(\cdot | \tau^i) \right) \right] \leq \frac{\delta}{N} \quad (16)$$

Then, we consider the original objective functions,

¹For the KL constraint, we assume that the sub-policies are independent.

$$\begin{aligned}
J^{MAPPO} &= \mathbb{E}_{\vec{a}_t, s_t \sim \pi_{\text{old}}} \left[\frac{\pi(\vec{a}_t | s_t)}{\pi_{\text{old}}(\vec{a}_t | s_t)} A^{\text{old}}(s_t, \vec{a}_t) \right] \\
&\approx \mathbb{E}_{\vec{a}_t, s_t \sim \pi_{\text{old}}} \left[\prod_i^N \frac{\pi^i(a_t^i | s_t^i)}{\pi_{\text{old}}^i(a_t^i | s_t^i)} A^{\text{old}}(s_t, \vec{a}_t) \right] \\
&\approx \mathbb{E}_{\vec{a}_t, s_t \sim \pi_{\text{old}}} \left[\prod_i^N \frac{\pi^i(a_t^i | \tau_t^i)}{\pi_{\text{old}}^i(a_t^i | \tau_t^i)} A^{\text{old}}(s_t, \vec{a}_t) \right]
\end{aligned} \quad (17)$$

and our surrogate objective functions,

$$\begin{aligned}
\widetilde{J^{MAPPO}} &= \mathbb{E}_{\vec{a}_t, s_t \sim \pi_{\text{old}}} \left[\frac{1}{N} \sum_i^N \frac{\pi^i(a_t^i | s_t^i)}{\pi_{\text{old}}^i(a_t^i | s_t^i)} A^{\text{old}}(s_t, \vec{a}_t) \right] \\
&\approx \frac{1}{N} \sum_i^N \mathbb{E}_{\vec{a}_t, s_t \sim \pi_{\text{old}}} \left[\frac{\pi^i(a_t^i | \tau_t^i)}{\pi_{\text{old}}^i(a_t^i | \tau_t^i)} A^{\text{old}}(s_t, \vec{a}_t) \right]
\end{aligned} \quad (18)$$

We prove that

$$\maximize \widetilde{J^{MAPPO}} \Rightarrow \maximize J^{MAPPO} \quad (19)$$

holds approximately with a small clip parameter ϵ in Appendix A. Intuitively, maximizing the size of item $\frac{\pi^i(a_t^i | s_t^i)}{\pi_{\text{old}}^i(a_t^i | s_t^i)} A^{\text{old}}(s_t, \vec{a}_t)$ for each agent $i \in N$ will also maximize the the size of item $\frac{\prod_i^N \pi^i(a_t^i | s_t^i)}{\prod_i^N \pi_{\text{old}}^i(a_t^i | s_t^i)} A^{\text{old}}(s_t, \vec{a}_t)$.

In practice, the joint policy of product form (in Eq. 13) may lead to numerical overflow and large variance with a large number of agents. The surrogate objective function (Eq. 18 and Eq. 16) has a better scalability and lower variance. And it allows us to optimize the independent policies of the agents with PPO-clip, called **vanilla Multi-agent PPO (MAPPO)**,

$$r^i = \frac{\pi^i(a^i | \tau^i)}{\pi_{\text{old}}^i(a^i | \tau^i)} \quad (20)$$

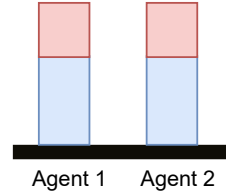
$$\begin{aligned}
J^{MAPPO-clip} &= \\
&\frac{1}{N} \sum_i^N \mathbb{E}_{\vec{a}_t, s_t \sim \pi_{\text{old}}} \left[\min \left(r^i A^{\text{old}}, \text{clip}(r^i, 1 - \epsilon, 1 + \epsilon) A^{\text{old}} \right) \right]
\end{aligned} \quad (21)$$

These simplified objective functions (Eq. 10 and Eq. 21) with a shared advantage value function make vanilla MAPPO and MAPG more scalable as well as easy to implement. Since there is no monotonicity constraint in the actor-critic methods, the expressiveness of vanilla MAPPO and MAPG is not limited. Besides, thanks to the architecture without a value mixing network, vanilla MAPPO and MAPG also do not have the problem of exploding the number of Q_i in QMIX.

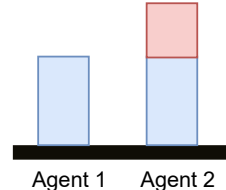
5 NOISY MAPPO

5.1 Motivation

In the previous section, we obtained the surrogate objective function of MAPPO with a centralized advantage function (or value function). Thus we can obtain the expected policy gradient for an agent $i \in N$,



(a) The stochastic policy gradient with the sampled shared advantage values.



(b) The true policy gradient.

Figure 2: These bar charts represents the action probability, and the red area indicates the amount of improvement of the probability by the policy gradient.

$$\begin{aligned}
\frac{\partial \hat{J}}{\partial \pi^i(a_t^i | s_t)} &\propto \mathbb{E}_{a_{\neq i} \sim \pi} [A^\pi(s_t, a_t^i, a_{\neq i}^{\neq i})] \\
&= \mathbb{E}_{a_{\neq i} \sim \pi} [r(s_t, a_t^i, a_{\neq i}^{\neq i}) + V(s_{t+1}) - V(s_t)]
\end{aligned} \quad (22)$$

this marginal advantage function can be seen as a **implicit multi-agent credit** [4, 18, 23] for agent i . In practice, MAPG and MAPPO estimate this gradient via sampling. Thus, according to the large number law, we need a large number of samples with the state s to estimate this expected gradient accurately. However, when the number of agents N is large, it is almost impossible for us to traverse the action space of all the agents in a batch of samples to obtain the true gradient. In addition, the bias of the approximate centralized value function is large at the beginning of the training. Therefore, in practice, we can usually only obtain the sampled mean gradient with deviations and large variance. These deviations may cause the policy of agent i to be updated in a sub-optimal direction, preventing the exploration of trajectories with higher returns. We call this problem: **The Policies Overfitting in Multi-agent Cooperation (POMAC)**.

To explain this problem more straightforwardly, we consider a multi-agent cooperative task with two agents. We assume that there is only one sample with reward r_t in a batch, and the advantage value

$$A^\pi(s_t, \vec{a}_t) := r_t + \gamma V^\pi(s_{t+1}) - V^\pi(s_t) \quad (23)$$

is obtained by agent two and is not related to agent one². The stochastic policy gradients with the this shared advantage value, i.e. $\frac{\partial \hat{J}}{\partial \pi^i(a_t^i | s_t)} \propto A^\pi(s_t, \vec{a}_t)$, may improve probabilities of the policies of both agents, shown in Figure 2a. But intuitively, the agent one's

²For example, agent one and agent two are far apart and agent two gets a reward r_t .

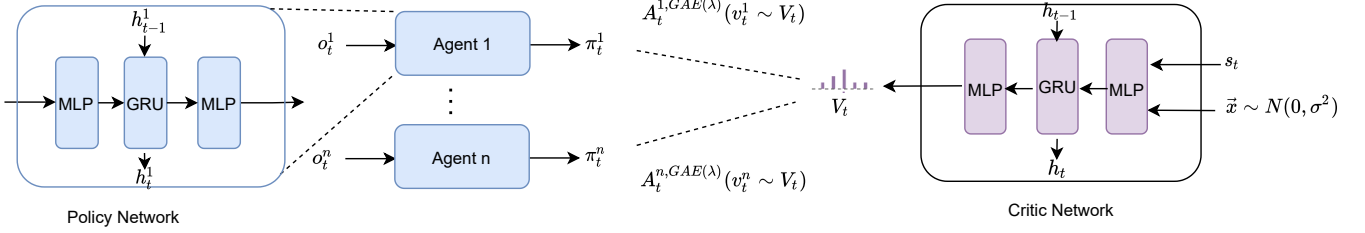


Figure 3: The framework of Noisy Value MAPPO (NV-MAPPO).

policy should not be updated as the advantage value is not related to agent one, shown in Figure 2b.

5.2 Noise Policy Perturbation

As the POMAC may cause MAPPO overfitting and converge to suboptimal solutions. In this section, we propose two novel noise-based policy perturbation methods to solve this problem.

Noisy-Advantage MAPPO (NA-MAPPO) demonstrated in Algo. 1 (Appendix B). We sample a fixed³ gaussian noise for each agent i ,

$$x^i \sim N(0, 1), \forall i \in N \quad (24)$$

where N is the number of agents. Next, we mix the advantage values A^b with these noises by a weight α (Eq. 25), perturbing the advantage values.

$$A_b^i = (1 - \alpha) \cdot A_b + \alpha \cdot x^i, \forall i \in N, b \in B \quad (25)$$

Noisy-Value MAPPO (NV-MAPPO) We randomly sample a gaussian noise vector $\bar{x}^i \sim N(0, \sigma^2)$ for each agent i , where σ^2 is the variance can be seen as the noise intensity (we fine-tune σ for each scenario, shown in Appendix C.2). We concatenate the noise \bar{x}^i with state s . Next, as shown in Figure 3, we feed the concatenated feature to the centralized value network to generate noise value v^i for each agent i ,

$$v^i = V(concat(s, \bar{x}^i)), \forall i \in N \quad (26)$$

The random noise \bar{x}^i disturbs the centralized value network. Then, the noise values of v^i propagate to the advantage value $A^i = r + \gamma v^i(s_{t+1}) - v^i(s_t)$ for each agent i , perturbing the advantage values. These advantage noises bring the following benefits,

- (1) the noises prevent the multi-agent policies over-fitting to the bias of the sampled advantage values.
- (2) the different noises x^i of each agent drive the multi-agent policies go in different directions, which encourage agents to explore diverse trajectories.
- (3) For the case where all agents share a policy network, the policies trained by N noisy value networks are similar to policies ensemble.

We then **combine the noise value function with vanilla MAPPO, MAPG, and IPPO** to propose NV-MAPPO, Noisy-Value

MAPG (NV-MAPG), and Noisy-Value IPPO (NV-IPPO), demonstrated in Algo. 2 (Appendix B). At last, we also show the difference between our method and MAPPO-FP in Table 1.

Algo.	MAPPO-FP	Noisy-MAPPO
Expert agent-specific features	Yes	No
Centralized Value-function	No	Yes
Noise	No	Yes
Theoretical analysis	No	Yes

Table 1: The difference between MAPPO-FP and Noisy-MAPPO.

6 EXPERIMENTS

In this section, we first evaluate the performance of NV-MAPPO, NA-MAPPO, and NV-IPPO in SMAC; and we analyze how these noises affect their performance and the entropy of the policies of MAPPO. We then evaluate the expressive power of NV-MAPPO on two non-monotonic matrix games.

6.1 Benchmark Environments

6.1.1 Starcraft Multi-agent Challenge (SMAC). [19] focuses on micromanagement challenges where each unit is controlled by an independent agent that must act based on local observations, which has become a common-used benchmark for evaluating state-of-the-art MARL approaches, such as [4, 14, 18, 22]. SMAC offers diverse sets of scenarios, which are classified as Easy, Hard, and Super Hard scenarios. We use the hardest scenarios in SMAC as our main benchmark environment.

6.1.2 Non-monotonic Matrix Game. [22] [14] show the non-monotonic matrix games that violates the monotonicity constraint. For the matrix game Table 3a (Sec. 6.3); in order to obtain the reward 8, both agents must select the first action 0 (actions are indexed from top to bottom, left to right); if only one agent selects action 0, they obtain reward -12. QMIX learns incorrect Q_{tot} in such non-monotonic matrix games [22] [14]. We use two payoff matrices (Sec. 6.3, Table 3a and 3b) to evaluate the expressive power of NV-MAPPO.

6.1.3 Evaluation Metric. Our primary evaluation metric is the function that maps the steps for the environment observed throughout the training to the median test-winning percentage/median test

³If we resample the noise for each episode, it will make the noise perturbation disappear, as the expectation of our gaussian noise is equal to zero.

Scenarios	Difficulty	NV-MAPPO	NA-MAPPO	NV-IPPO	vanilla MAPPO	MAPPO-FP	IPPO	Fine-tuned QMIX
2s3z	Easy	100%	-	-	100%	100%	100%	100%
1c3s5z	Easy	100%	-	-	100%	100%	100%	100%
3s5z	Easy	100%	-	-	100%	100%	100%	100%
2s_vs_1sc	Easy	100%	-	-	100%	100%	100%	100%
3s_vs_5z	Hard	100%	100%	100%	98%	100%	100%	100%
2c_vs_64zg	Hard	100%	100%	100%	100%	100%	98%	100%
5m_vs_6m	Hard	89%	85%	87%	25%	89%	87%	90%
8m_vs_9m	Hard	96%	96%	96%	93%	96%	96%	100%
MMM2	Super Hard	96%	96%	86%	96%	90%	86%	100%
3s5z_vs_3s6z	Super Hard	87%	72%	96%	56%	84%	82%	75%(env=8)
6h_vs_8z	Super Hard	91%	90%	94%	15%	88%	84%	91%
corridor	Super Hard	100%	100%	98%	3%	100%	98%	100%
27m_vs_30m	Super Hard	100%	98%	72%	98%	94%	69%	100%
Avg. Score	Hard+	95.5%	93.2%	91.9 %	64.9%	93.4%	88.8%	95.1%

Table 2: Median test win percentage of MARL algorithms in all scenarios.

The test results for MAPPO-FP and IPPO are from [26].

return of the evaluation. Just as in QMIX [18], we repeat each experiment with several independent training runs (five independent random experiments).

6.2 SMAC

In this section, we evaluate the performance of the algorithms on SMAC. We test our noisy value function on MAPPO and IPPO, i.e., NV-MAPPO nad NV-IPPO, respectively, in SMAC. We use the Fine-tuned QMIX [5] and MAPPO-FP as the baseline, as they achieve SOTA performance in SMAC among the previous works; we do not compare NV-MAPPO with MADDPG as the past experiments [17, 27] shows that it does not perform well under SMAC.

6.2.1 Performance Comparison. The experimental results in Table 2 demonstrate that (1) **The performance of NV-MAPPO significantly exceeds that of vanilla MAPPO** on most hard scenarios, such as 5m_vs_6m (+65%), corridor (+97%), 6h_vs_8z (+87%) and 3s5z_vs_3s6z (+31%). (2) NV-IPPO achieves extraordinarily high win rates in Super Hard scenarios 3s5z_vs_3s6z (96%) and 6h_vs_8z (94%); we speculate that this is because the noise also prevents IPPO from overfitting due to non-stationarity. (3) The average performance of NV-MAPPO on hard scenarios is better than that of Fine-tuned QMIX and MAPPO-FP. (4) We compare MAPG and NV-MAPG in the Appendix C.1 and find that NV-MAPG also performs significantly better than MAPG.

All these results indicate that the noisy value function works well in practical tasks. Since we use Fine-tuned QMIX [5] as the baseline, the median test-winning rates of QMIX are significantly better than the experimental results in the past literature [14, 18, 19, 25]. So far, **NV-MAPPO and NV-IPPO together achieve SOTA in SMAC**. Specifically, NV-IPPO (3s5z_vs_3s6z and 6h_vs_8z) and NV-MAPPO (other scenarios) have an **average win rate of 97% for all hard scenarios**.

6.2.2 Comparing NA-MAPPO with NV-MAPPO. In previous sections, We have proposed two noise-based methods, i.e, NA-MAPPO with NV-MAPPO, to resolve the POMAC. In this section, we compare their performance in SMAC. As shown in Figure 4, we find that

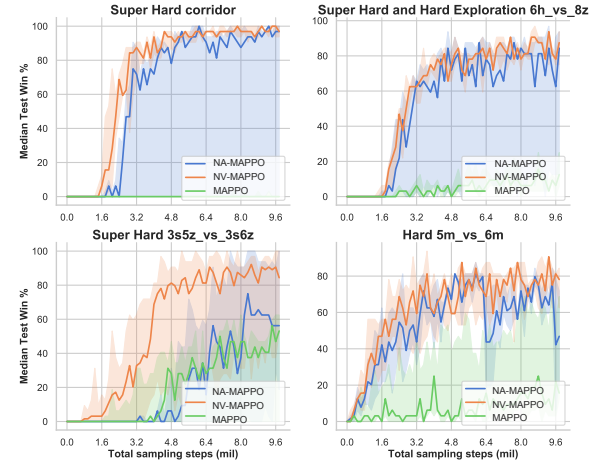


Figure 4: Comparing Noisy-Advantage MAPPO (NA-MAPPO) with Noisy-Value MAPPO (NV-MAPPO). The win rates of Noisy-Advantage MAPPO have a large variance.

the Advantage-Noisy method may harm the stability of the algorithm in some scenarios, i.e, **the win rates of Noisy-Advantage methods have a large variance**. We speculate that it may be the explicit noises destroy the original direction of the policy gradient. However, the performance of the NA-MAPPO is still comparable to NV-MAPPO in some hard scenarios of SMAC; and we note that the NA-MAPPO is extremely easy to implement. All of these results indicate the noise advantage values do improve the performance of vanilla MAPPO.

6.2.3 Analysis of the Variance of v^i . Next, we perform further experimental analysis on how the noisy value function of NV-MAPPO affects the performance. We show the standard deviation of the value function v^i in agent dimension for some Hard scenarios in Figure 5. We find that **the large variance of v^i in some scenarios implies that the performance improvement of NV-MAPPO**

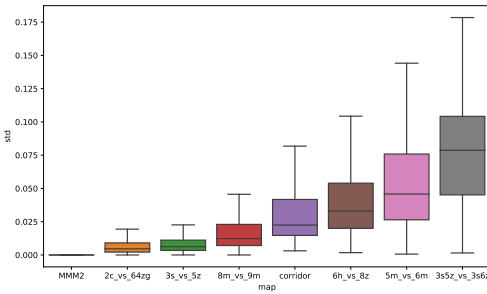


Figure 5: The standard deviation of noisy value function v^i in the agent dimension.

The figure shows that scenarios with larger variance of v^i imply that noise also has a significant performance improvement on them.

over vanilla MAPPO in these scenarios is also large, such as 3s5z_vs_3s6z and 6h_vs_8z (see Figure 5 and Figure 4). This law reveals that the performance improvement of NV-MAPPO does come from noise perturbation of value function.

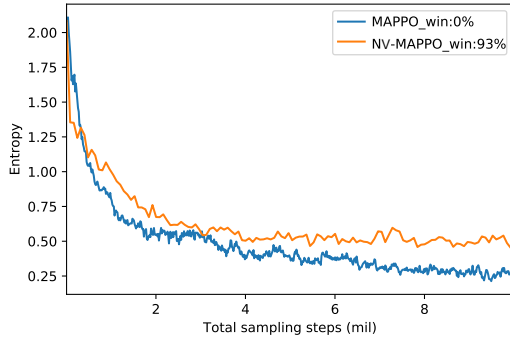


Figure 6: The average entropy of the policies of vanilla MAPPO and NV-MAPPO.

6.2.4 Analysis of Policy Entropy. Finally we analyze the effect of the noisy value function on the entropy of the policies on scenario 3s5z_vs_3s6z. As shown in Figure 6, the entropy of vanilla MAPPO’s policies drops rapidly and falls into the local optimal solution, thus the winning rate is always zero. As for NV-MAPPO, we smoothed the sampled advantage values and the noise prevents policies overfitting, thus the entropy of the policies decreases more cautiously.

6.3 Non-monotonic Matrix Game

In this section, we evaluate the expressiveness of NV-MAPPO using two non-monotonic matrix games; As shown in Figure 7a and 7b, since there are no constraints on the value function of MAPPO (e.g., monotonicity constraints), the test performance of NV-MAPPO in both of these non-monotonic games are significantly better than

QMIX. Since we use the Fine-tuned QMIX, the test returns of QMIX in matrix 3b is better than that in the past literature [14].

8	-12	-12
-12	0	0
-12	0	0

(a) Payoff matrix 1

12	0	10
0	10	10
10	10	10

(b) Payoff matrix 2

Table 3: Non-monotonic matrix games from [22] (a) and [14](b)

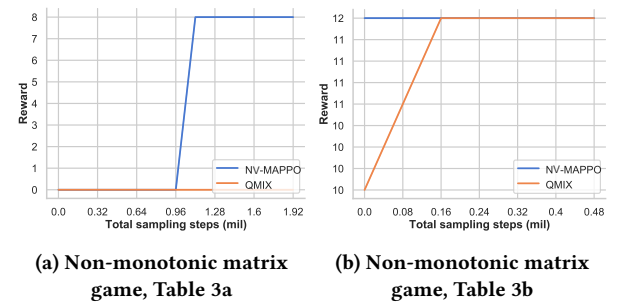


Figure 7: Test returns for non-monotonic matrix games from Sec.6.3

7 CONCLUSION

In this paper, we extend the single-agent PG and PPO algorithms to MAPG and MAPPO algorithms with theoretical analysis. Then, to solve the POMAC problem in MAPG and vanilla MAPPO, we propose two noisy advantage-value methods (NV-MAPPO and NA-MAPPO). The experimental results show that NV-MAPPO and NV-IPPO together achieve extraordinarily high win rates in all scenarios and achieve SOTA in SMAC, without limitation of expressiveness and artificial agent-specific features. Our work demonstrates that the perturbation of policies with noisy advantage values effectively improves the performance of the multi-agent actor-critic algorithms.

REFERENCES

[1] Yongcan Cao, Wenwu Yu, Wei Ren, and Guanrong Chen. 2012. An overview of recent progress in the study of distributed multi-agent coordination. *IEEE Transactions on Industrial informatics* 9, 1 (2012), 427–438.

[2] Yu-Han Chang, Tracey Ho, and Leslie P Kaelbling. 2004. All learning is local: Multi-agent learning in global reward games. (2004).

[3] Christian Schroeder de Witt, Tarun Gupta, Denys Makoviichuk, Viktor Makoviychuk, Philip HS Torr, Mingfei Sun, and Shimon Whiteson. 2020. Is Independent Learning All You Need in the StarCraft Multi-Agent Challenge? *arXiv preprint arXiv:2011.09533* (2020).

[4] Jakob N. Foerster, Gregory Farquhar, Triantafyllos Afouras, Nantas Nardelli, and Shimon Whiteson. 2018. Counterfactual Multi-Agent Policy Gradients. In *Proceedings of the Thirty-Second AAAI Conference on Artificial Intelligence (AAAI-18), the 30th innovative Applications of Artificial Intelligence (IAAI-18), and the 8th AAAI Symposium on Educational Advances in Artificial Intelligence (EAAI-18), New Orleans, Louisiana, USA, February 2-7, 2018*, Sheila A. McIlraith and Kilian Q. Weinberger (Eds.). AAAI Press, 2974–2982. <https://www.aaai.org/ocs/index.php/AAAI/AAAI18/paper/view/17193>

[5] Jian Hu, Siyang Jiang, Seth Austin Harding, Haibin Wu, and Shih-wei Liao. 2021. Rethinking the Implementation Tricks and Monotonicity Constraint in Cooperative Multi-Agent Reinforcement Learning. *arXiv preprint arXiv:2102.03479* (2021).

[6] Maximilian Hüttenrauch, Adrian Šošić, and Gerhard Neumann. 2017. Guided deep reinforcement learning for swarm systems. *arXiv preprint arXiv:1709.06011* (2017).

[7] Shariq Iqbal and Fei Sha. 2019. Actor-Attention-Critic for Multi-Agent Reinforcement Learning. In *Proceedings of the 36th International Conference on Machine Learning, ICML 2019, 9-15 June 2019, Long Beach, California, USA (Proceedings of Machine Learning Research, Vol. 97)*, Kamalika Chaudhuri and Ruslan Salakhutdinov (Eds.). PMLR, 2961–2970. <http://proceedings.mlr.press/v97/iqbal19a.html>

[8] Sham M Kakade. 2001. A natural policy gradient. *Advances in neural information processing systems* 14 (2001).

[9] Diederik P. Kingma and Jimmy Ba. 2015. Adam: A Method for Stochastic Optimization. In *3rd International Conference on Learning Representations, ICLR 2015, San Diego, CA, USA, May 7-9, 2015, Conference Track Proceedings*, Yoshua Bengio and Yann LeCun (Eds.). <http://arxiv.org/abs/1412.6980>

[10] Landon Kraemer and Bikramjit Banerjee. 2016. Multi-Agent Reinforcement Learning as a Rehearsal for Decentralized Planning. *Neurocomputing* 190 (2016), 82–94. <https://doi.org/10.1016/j.neucom.2016.01.031>

[11] Hepeng Li and Haibo He. 2020. Multi-Agent Trust Region Policy Optimization. *arXiv preprint arXiv:2010.07916* (2020).

[12] Timothy P. Lillicrap, Jonathan J. Hunt, Alexander Pritzel, Nicolas Heess, Tom Erez, Yuval Tassa, David Silver, and Daan Wierstra. 2016. Continuous control with deep reinforcement learning. In *4th International Conference on Learning Representations, ICLR 2016, San Juan, Puerto Rico, May 2-4, 2016, Conference Track Proceedings*, Yoshua Bengio and Yann LeCun (Eds.). <http://arxiv.org/abs/1509.02971>

[13] Ryan Lowe, Yi Wu, Aviv Tamar, Jean Harb, Pieter Abbeel, and Igor Mordatch. 2017. Multi-Agent Actor-Critic for Mixed Cooperative-Competitive Environments. In *Advances in Neural Information Processing Systems 30: Annual Conference on Neural Information Processing Systems 2017, December 4-9, 2017, Long Beach, CA, USA*, Isabelle Guyon, Ulrike von Luxburg, Samy Bengio, Hanna M. Wallach, Rob Fergus, S. V. N. Vishwanathan, and Roman Garnett (Eds.). 6379–6390. <https://proceedings.neurips.cc/paper/2017/hash/68a9750337a418a86fe06c1991a1d64c-Abstract.html>

[14] Anuj Mahajan, Tabish Rashid, Mikayel Samvelyan, and Shimon Whiteson. 2019. MAVEN: Multi-Agent Variational Exploration. In *Advances in Neural Information Processing Systems 32: Annual Conference on Neural Information Processing Systems 2019, NeurIPS 2019, December 8-14, 2019, Vancouver, BC, Canada*, Hanna M. Wallach, Hugo Larochelle, Alina Beygelzimer, Florence d’Alché-Buc, Emily B. Fox, and Roman Garnett (Eds.). 7611–7622. <https://proceedings.neurips.cc/paper/2019/hash/f816dc0acfacc7498e10496222e9db10-Abstract.html>

[15] Volodymyr Mnih, Adrià Puigdomènech Badia, Mehdi Mirza, Alex Graves, Timothy P. Lillicrap, Tim Harley, David Silver, and Koray Kavukcuoglu. 2016. Asynchronous Methods for Deep Reinforcement Learning. In *Proceedings of the 33nd International Conference on Machine Learning, ICML 2016, New York City, NY, USA, June 19-24, 2016 (JMLR Workshop and Conference Proceedings, Vol. 48)*, Maria-Florina Balcan and Kilian Q. Weinberger (Eds.). JMLR.org, 1928–1937. <http://proceedings.mlr.press/v48/mnih16.html>

[16] Sylvie CW Ong, Shao Wei Png, David Hsu, and Wee Sun Lee. 2009. POMDPs for robotic tasks with mixed observability. 5 (2009), 4.

[17] Bei Peng, Tabish Rashid, Christian A Schroeder de Witt, Pierre-Alexandre Kamenny, Philip HS Torr, Wendelin Böhmer, and Shimon Whiteson. 2020. FACMAC: Factored Multi-Agent Centralised Policy Gradients. *arXiv e-prints* (2020), arXiv-2003.

[18] Tabish Rashid, Mikayel Samvelyan, Christian Schröder de Witt, Gregory Farquhar, Jakob N. Foerster, and Shimon Whiteson. 2018. QMIX: Monotonic Value Function Factorisation for Deep Multi-Agent Reinforcement Learning. In *Proceedings of the 35th International Conference on Machine Learning, ICML 2018, Stockholm, Sweden, July 10-15, 2018 (Proceedings of Machine Learning Research, Vol. 80)*, Jennifer G. Dy and Andreas Krause (Eds.). PMLR, 4292–4301. <http://proceedings.mlr.press/v80/rashid18a.html>

[19] Mikayel Samvelyan, Tabish Rashid, Christian Schroeder de Witt, Gregory Farquhar, Nantas Nardelli, Tim G. J. Rudner, Chia-Man Hung, Philip H. S. Torr, Jakob Foerster, and Shimon Whiteson. 2019. The StarCraft Multi-Agent Challenge. *arXiv preprint arXiv:1902.04043* (2019).

[20] John Schulman, Sergey Levine, Pieter Abbeel, Michael Jordan, and Philipp Moritz. 2015. Trust region policy optimization. In *International conference on machine learning*. PMLR, 1889–1897.

[21] John Schulman, Filip Wolski, Prafulla Dhariwal, Alec Radford, and Oleg Klimov. 2017. Proximal policy optimization algorithms. *arXiv preprint arXiv:1707.06347* (2017).

[22] Kyunghwan Son, Daewoo Kim, Wan Ju Kang, David Hostallero, and Yung Yi. 2019. QTRAN: Learning to Factorize with Transformation for Cooperative Multi-Agent Reinforcement Learning. In *Proceedings of the 36th International Conference on Machine Learning, ICML 2019, 9-15 June 2019, Long Beach, California, USA (Proceedings of Machine Learning Research, Vol. 97)*, Kamalika Chaudhuri and Ruslan Salakhutdinov (Eds.). PMLR, 5887–5896. <http://proceedings.mlr.press/v97/son19a.html>

[23] Peter Sunehag, Guy Lever, Audrunas Gruslys, Wojciech Marian Czarnecki, Vincius Zambaldi, Max Jaderberg, Marc Lanctot, Nicolas Sonnerat, Joel Z. Leibo, Karl Tuyls, and Thore Graepel. 2017. Value-Decomposition Networks For Cooperative Multi-Agent Learning. *arXiv preprint arXiv:1706.05296* (2017).

[24] Ming Tan. 1993. Multi-agent reinforcement learning: Independent vs. cooperative agents. In *Proceedings of the tenth international conference on machine learning*. 330–337.

[25] Yaodong Yang, Jianye Hao, Ben Liao, Kun Shao, Guangyong Chen, Wulong Liu, and Hongyao Tang. 2020. Qatten: A General Framework for Cooperative Multiagent Reinforcement Learning. *arXiv preprint arXiv:2002.03939* (2020).

[26] Chao Yu, Akash Veliu, Eugene Vinitsky, Yu Wang, Alexandre Bayen, and Yi Wu. 2021. The surprising effectiveness of mappo in cooperative, multi-agent games. *arXiv preprint arXiv:2103.01955* (2021).

[27] Meng Zhou, Ziyu Liu, Pengwei Sui, Yixuan Li, and Yuk Ying Chung. 2020. Learning Implicit Credit Assignment for Multi-Agent Actor-Critic. *arXiv preprint arXiv:2007.02529* (2020).

A ANALYSIS OF VANILLA MAPPO

Definition A.1. Original objective function:

$$\begin{aligned} J^{\text{MAPPO}} &= \mathbb{E}_{\tau \sim \mathcal{D}} \left[\frac{\pi(\vec{a}_t | s_t)}{\pi_{\text{old}}(\vec{a}_t | s_t)} A_t^{\text{old}}(s_t, \vec{a}_t) \right] \\ &= \mathbb{E}_{\tau \sim \mathcal{D}} \left[\prod_i^N \frac{\pi^i(a_t^i | s_t)}{\pi_{\text{old}}^i(a_t^i | s_t)} A_t^{\text{old}}(s_t, \vec{a}_t) \right] \end{aligned}$$

Surrogate objective function:

$$\hat{J^{\text{MAPPO}}} = \mathbb{E}_{\tau \sim \mathcal{D}} \left[\frac{1}{N} \sum_i^N \frac{\pi^i(a_t^i | s_t)}{\pi_{\text{old}}^i(a_t^i | s_t)} A_t^{\text{old}}(s_t, \vec{a}_t) \right]$$

where \mathcal{D} is the trajectories sampled by joint policy π^{old} , and N is the number of agents.

In this section, we prove that

$$\text{maximize } \hat{J^{\text{MAPPO}}} \Rightarrow \text{maximize } J^{\text{MAPPO}} \quad (27)$$

holds approximately with following **constraints**,

- (1) Clip constraint: $1 - \epsilon \leq \frac{\pi^i(\cdot | s_t)}{\pi_{\text{old}}^i(\cdot | s_t)} \leq 1 + \epsilon$, where ϵ is the clip parameter; We use this constraint to approximate the KL divergence constraint.
- (2) Probability constraint: $\sum_{k=1}^{|\mathcal{K}|} \pi^i(a_t^{i,k} | s_t) = 1$, where \mathcal{K} denotes all actions of the agent.

PROOF. We know that that maximizing surrogate objective function $\hat{J^{\text{MAPPO}}}$ is equivalent to,

- (1) Maximizing the invidual ratio for each agent $\frac{\pi^i(a_t^i | s_t)}{\pi_{\text{old}}^i(a_t^i | s_t)}$ for each item in $\hat{J^{\text{MAPPO}}}$ that $A_t^{\text{old}} > 0$.
- (2) Minimizing the invidual ratio for each agent $\frac{\pi^i(a_t^i | s_t)}{\pi_{\text{old}}^i(a_t^i | s_t)}$ for each item in $\hat{J^{\text{MAPPO}}}$ that $A_t^{\text{old}} < 0$.

and maximizing original objective function J^{MAPPO} is equivalent to,

- (1) Maximizing the joint ratio $\prod_i^N \frac{\pi^i(a_t^i | s_t)}{\pi_{\text{old}}^i(a_t^i | s_t)}$ for each item in J^{MAPPO} that $A_t^{\text{old}} > 0$.
- (2) Minimizing the joint ratio $\prod_i^N \frac{\pi^i(a_t^i | s_t)}{\pi_{\text{old}}^i(a_t^i | s_t)}$ for each item in J^{MAPPO} that $A_t^{\text{old}} < 0$.

Due to the probability constraint, the above problems can be equated as: **transferring the action probability of the items with small advantage value A^{small} to the items with large advantage value A^{large} .**

Given that $\pi^* = \arg \max_{\pi} \hat{J^{\text{MAPPO}}}$, and there exists

$$\pi' = \arg \max_{\pi} J^{\text{MAPPO}} \neq \pi^* \text{ and } J^{\text{MAPPO}}_{\pi'} > J^{\text{MAPPO}}_{\pi^*}$$

which means that there are some action probability transfers between π^* and π' : e.g, given a pair of items with the same state s and different actions \vec{a} and \vec{a}' , in the original objective function $J^{\text{MAPPO}}_{\pi^*}$,

$$\frac{\pi^{j,*}(a^j | s)}{\pi_{\text{old}}^j(a^j | s)} \cdot \prod_{i \neq j}^N \frac{\pi^{i,*}(a^i | s)}{\pi_{\text{old}}^i(a^i | s)} A_t^{\text{old}}(s, \vec{a}) \quad (28)$$

$$\frac{\pi^{j,*}(a^{j'} | s)}{\pi_{\text{old}}^j(a^{j'} | s)} \cdot \prod_{i \neq j}^N \frac{\pi^{i,*}(a^{i'} | s)}{\pi_{\text{old}}^i(a^{i'} | s)} A_t^{\text{old}}(s, \vec{a}') \quad (29)$$

π' can transfer the action probability of $\pi^{j,*}(a^{j'} | s)$ to $\pi^{j,*}(a^j | s)$ to make that $J^{\text{MAPPO}}_{\pi'} > J^{\text{MAPPO}}_{\pi^*}$ with following conditions hold for above two items,

- (1) $\frac{A_t^{\text{old}}(s, \vec{a})}{\pi_{\text{old}}^j(a^j | s)} \prod_{i \neq j}^N \frac{\pi^{i,*}(a^i | s)}{\pi_{\text{old}}^i(a^i | s)} > \frac{A_t^{\text{old}}(s, \vec{a}')}{\pi_{\text{old}}^j(a^{j'} | s)} \prod_{i \neq j}^N \frac{\pi^{i,*}(a^{i'} | s)}{\pi_{\text{old}}^i(a^{i'} | s)}$; this allows the transfer of probabilities to increase the size of the sum of above a pair items.
- (2) Clip constraint: $\frac{\pi^{j,*}(a^j | s)}{\pi_{\text{old}}^j(a^j | s)} < 1 + \epsilon$ and $\frac{\pi^{j,*}(a^{j'} | s)}{\pi_{\text{old}}^j(a^{j'} | s)} > 1 - \epsilon$.

As π^* is a optimal solution of $\hat{J^{\text{MAPPO}}}_{\pi^*}$, we obtain that

- (1) $\frac{A_t^{\text{old}}(s, \vec{a})}{\pi_{\text{old}}^j(a^j | s)} \leq \frac{A_t^{\text{old}}(s, \vec{a}')}{\pi_{\text{old}}^j(a^{j'} | s)}$; if this inequality does not hold, we can obtain that $J^{\text{MAPPO}}_{\pi'} > J^{\text{MAPPO}}_{\pi^*}$ with the action probability transfer from $\pi^{j,*}(a^{j'} | s)$ to $\pi^{j,*}(a^j | s)$, which contradicts that π^* is the optimal solution of $\hat{J^{\text{MAPPO}}}_{\pi^*}$. As the $A_t^{\text{old}}(s, \vec{a})$ determines the sign of the entire ratios items, this inequality implies that condition (1) can only hold if $A_t^{\text{old}}(s, \vec{a})$ and $A_t^{\text{old}}(s, \vec{a}')$ have the same sign. Thus the probability of the condition (1) holds is small.
- (2) By the previous equivalence problem of maximizing $\hat{J^{\text{MAPPO}}}_{\pi^*}$, we can see that most of the action probability ratios of π^* may approach the boundary of the clip constraint with a small ϵ . This implies that the probability of above condition (2) holds is small.

Thus we assume that above strict conditions hold with a **small probability** η for a ratio item $\frac{\pi^{j,*}(a^j | s)}{\pi_{\text{old}}^j(a^j | s)}$ where $j \in N$. Then, π' can only transfer the actions probability of $|\mathcal{D}| \cdot N \cdot \eta$ ratio items of $J^{\text{MAPPO}}_{\pi^*}$ to increase the size of it. Next, we obatined that

$$\frac{J^{\text{MAPPO}}_{\pi'}}{J^{\text{MAPPO}}_{\pi^*}} \approx \frac{|\mathcal{D}| \cdot [(1+C)^{\eta \cdot N}]}{|\mathcal{D}| \cdot 1} = (1+C)^{\eta \cdot N} \quad (30)$$

where C is the average lift size of the ratio items in $J^{\text{MAPPO}}_{\pi^*}$ for a pair of action probability transfer; and C is a small value due to (1) most of the action probability ratios of π^* may approach the boundary of the clip constraint with a small ϵ ; (2) $A_t^{\text{old}}(s, \vec{a})$ and $A_t^{\text{old}}(s, \vec{a}')$ have the same sign, which makes that the probability transfer to increase the size of one item while decreasing the size of the other.

Finally, we see that π^* is close to π' with a gap (Eq.30); and as the small clip hyperparameter ϵ implies the η and C are also small, the **gap is small when ϵ is a small value**. \square

B PSEUDOCODE

Algo. 2 and Algo. 1 demonstrate NV-MAPPO and NA-MAPPO, respectively. NV-MAPPO adds Gaussian noise to the input layer of

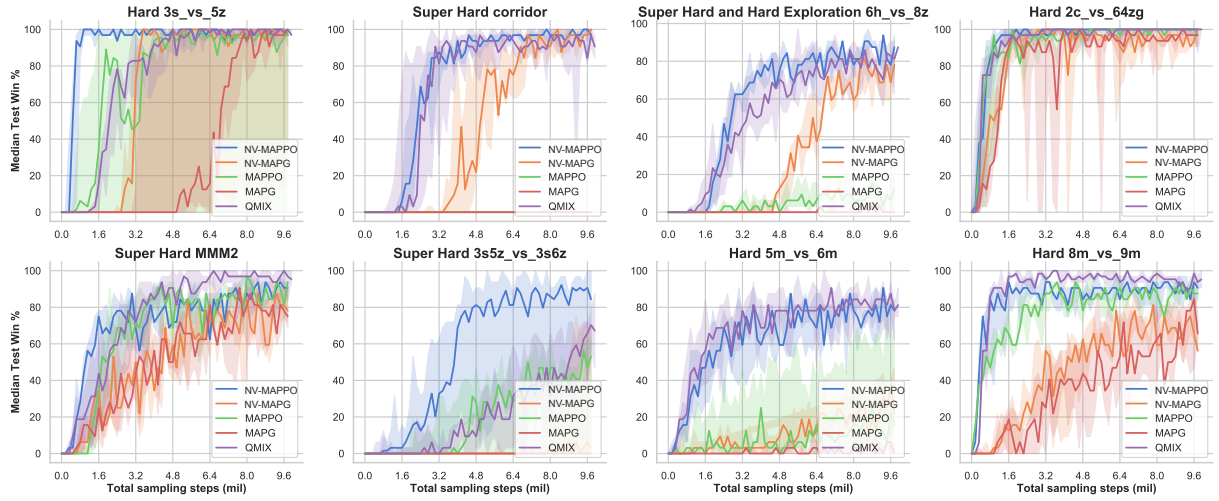


Figure 8: Median test win rate of MARL algorithms on hard scenarios in SMAC.
NV denotes Noisy-Value

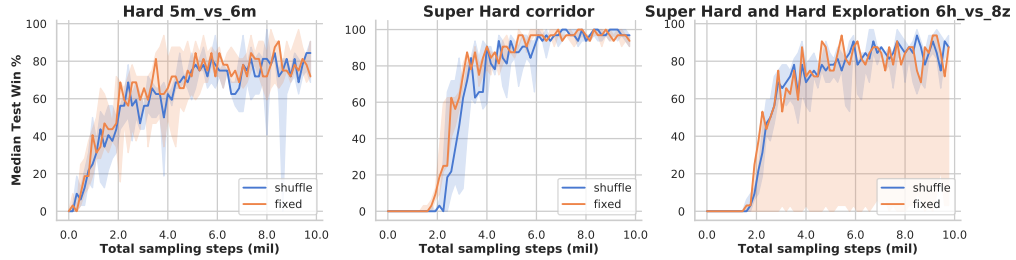


Figure 9: The performance comparison of fixed noise vectors and shuffle noise vectors (every 100 episodes).

the Value Network, and NA-MAPPO adds Gaussian noise directly to the normalized advantage values.

C EXPERIMENTAL DETAILS

C.1 Ommited Figures

Here, we echo the experiments in Sec. 6. Figure 8 shows the experimental results for Fine-tuned QMIX, MAPPO, MAPG, NV-MAPPO and NV-MAPG, which demonstrates the performance gains from noise (MAPG vs NV-MAPG, MAPPO vs NV-MAPPO).

C.2 Hyperparameters

Our hyperparameters are heavily based on recent papers [26] and [5], who fine-tune PPO⁴ and QMIX⁵, respectively, to make them work well in complex multi-agent tasks, such as SMAC. Table 4 shows the common hyperparameters of QMIX and MAPPO. Table 5 shows the hyperparameters of NV-MAPPO and NA-MAPPO for each scenarios, where the values of σ and α are depend on the scenarios.

For the **noise shuffle interval** of NV-MAPPO, we find that the performance of the fixed gaussian noise vectors x^i is comparable

to that of the noise of periodic shuffle (100 episodes), as shown in Figure 9. Note that this fixed noise vector cannot be seen as an identifier for an agent, as the value network cannot infer that which agent it is just by a noise vector \vec{x} and state s (unless you also feeds the observation o^i of the agent, likewise MAPPO-FP).

Other settings For the non-monotonic matrix games, we set the number of environments of all algorithms to 32, buffer length to 1, noise vector dim to 10, training epochs to 10, and σ to 1. At last, we use StarCraft 2 (SC2.4.10) in the latest PyMARL in our experiments.

⁴PPO Code: <https://github.com/marlbenchmark/on-policy>

⁵QMIX code: <https://github.com/hijkzzz/pymarl2>

hyperparameters	MAPPO and MAPG	QMIX
num envs	8	8
buffer length	400	-
batch size(episodes)	-	128
num GRU layers	1	1
RNN hidden state dim	64	64
fc layer dim	64	64
num fc before RNN	1	1
num fc after RNN	1	1
num noise dim	10	-
Adam [9] lr	5e-4	1e-3
$Q(\lambda)$	-	0.6, (0.3 for 6h_vs_8z)
GAE(λ)	0.95	-
entropy coef	0.01	-
PPO clip	0.2	-
noise shuffle interval (episodes)	$+\infty$	-
ϵ anneal steps	-	100k, (500k for 6h_vs_8z)

Table 4: Common hyperparameters used in the SMAC domain for all algorithms.

map	PPO epochs	mini-batch	gain	network	stacked frames	NV-MAPPO	NV-MAPG	NV-IPPO	NA-MAPPO
						σ	σ	σ	α
2s3z	15	1	0.01	rnn	1	1	1	-	-
1c3s5z	15	1	0.01	rnn	1	1	1	-	-
3s5z	5	1	0.01	rnn	1	1	1	-	-
2s_vs_1sc	15	1	0.01	rnn	1	1	1	-	-
3s_vs_5z	15	1	0.01	mlp	4	1	1	1	0.05
2c_vs_64zg	5	1	0.01	rnn	1	1	1	1	0.05
5m_vs_6m	8	1	0.01	rnn	1	8	3	0	0.05
8m_vs_9m	15	1	0.01	rnn	1	1	0.05	1	0.05
corridor	5	1	0.01	mlp	1	3	1	1	0.06
MMM2	5	2	1	rnn	1	0	0.5	0	0
3s5z_vs_3s6z	5	1	0.01	rnn	1	10	1	8	0.05
6h_vs_8z	5	3	0.01	mlp	1	1	1	1	0.06
27m_vs_30m	5	1	0.01	rnn	1	1	1	1	0

Table 5: Hyperparameters for NV-MAPPO, NA-MAPPO, NV-IPPO, NV-MAPG and vanilla MAPPO in SMAC.

Algorithm 1: NA-MAPPO

input :Initialize parameters $\theta; \phi$; $\mathcal{D} \leftarrow \{\}$; batch size B ; N agents; noise weight α ; entropy loss weight η ; λ for GAE(λ);

1 Sample Gaussian noise $x^i \sim \mathcal{N}(0, 1)$, $\forall i \in N$;
2 **for** each episodic iteration **do**
3 **for** episodic step t **do**
4 $\vec{a}_t = [\pi_\theta^i(o_t^i), \forall i \in N]$;
5 Execute actions \vec{a}_t , observe r_t, s_{t+1}, o_{t+1} ;
6 $\mathcal{D} \leftarrow \mathcal{D} \cup \mathcal{D}\{(s_t, \vec{o}_t, \vec{a}_t, r_t, s_{t+1}, o_{t+1}, \}_{t=1}^T\}$;
7 **end**
8 Sample random batch B from \mathcal{D} ;
9 Compute advantage $\hat{A}_1, \dots, \hat{A}_b$ and returns $\hat{R}_1, \dots, \hat{R}_b$ via GAE(λ);
10 then mixing the noise with the normalized advantage values:
11

$$\hat{A}_b^i = (1 - \alpha)\hat{A}_b + \alpha \cdot x^i, \forall i \in N, b \in B$$

12 **for** each training epochs **do**
13 Update critic by minimizing the loss $L(\phi)$;
14
15
$$L(\phi) = \frac{1}{B} \sum_{b=1}^B (v_b(\phi) - \hat{R}_b)^2$$

16 Update policy by using loss $L(\theta)$;
17
18
$$r_b^i(\theta) = \frac{\pi_\theta^i(a_b^i | o_b^i)}{\pi_{\theta_{old}}^i(a_b^i | o_b^i)}, \forall i \in N, b \in B$$

19
$$L(\theta) = \frac{1}{B \cdot N} \sum_{b=1}^B \sum_{i=1}^N [\min(r_b^i(\theta) \hat{A}_b^i, \text{clip}(r_b^i(\theta), 1 - \epsilon, 1 + \epsilon) \hat{A}_b^i) - \eta \mathcal{H}(\pi_\theta^i(o_b^i))]$$

20 where \mathcal{H} is the Shannon Entropy.
21 **end**
22 **end**

Algorithm 2: NV-MAPPO

input :Initialize parameters $\theta; \phi$; $\mathcal{D} \leftarrow \{\}$; batch size B ; N agents; noise variance σ^2 ; entropy loss weight η ; λ for GAE(λ);

1 Sample random noise vectors \vec{x}^i for each agent, $\vec{x}^i \sim \mathcal{N}(0, \sigma^2)$, $\forall i \in N$;
2 **for** each episodic iteration **do**
3 **for** episodic step t **do**
4 $\vec{a}_t = [\pi_\theta^i(o_t^i), \forall i \in N]$;
5 Execute actions \vec{a}_t , observe r_t, s_{t+1}, o_{t+1} ;
6 $\mathcal{D} \leftarrow \mathcal{D} \cup \mathcal{D}\{(s_t, \vec{o}_t, \vec{a}_t, r_t, s_{t+1}, o_{t+1}, \}_{t=1}^T\}$;
7 **end**
8 **if** at noise vectors shuffle interval **then**
9 | Shuffle the noise vectors \vec{x}^i in agent dimension.
10 **end**
11 Sample random batch B from \mathcal{D} ;
12 Noise value function forward for each agent, $v_b^i(\phi) = V_\phi(\text{concat}(s_b, \vec{x}^i))$, $\forall i \in N, b \in B$;
13 Compute advantage $\hat{A}_1^i, \dots, \hat{A}_b^i$ and returns $\hat{R}_1^i, \dots, \hat{R}_b^i$ via GAE(λ) with $v_b^i(\phi)$, $\forall i \in N, b \in B$;
14 **for** each training epochs **do**
15 Update critic by minimizing the loss $L(\phi)$;
16
17
$$L(\phi) = \frac{1}{B \cdot N} \sum_{i=1}^N \sum_{b=1}^B (v_b^i(\phi) - \hat{R}_b^i)^2$$

18 Update policy by using loss $L(\theta)$;
19
20
$$r_b^i(\theta) = \frac{\pi_\theta^i(a_b^i | o_b^i)}{\pi_{\theta_{old}}^i(a_b^i | o_b^i)}, \forall i \in N, b \in B$$

21
$$L(\theta) = \frac{1}{B \cdot N} \sum_{b=1}^B \sum_{i=1}^N [\min(r_b^i(\theta) \hat{A}_b^i, \text{clip}(r_b^i(\theta), 1 - \epsilon, 1 + \epsilon) \hat{A}_b^i) - \eta \mathcal{H}(\pi_\theta^i(o_b^i))]$$

22 where \mathcal{H} is the Shannon Entropy.
23 **end**
24 **end**
